

Article

Kinetic Research on the Curing Reaction of Hydroxyl-Terminated Polybutadiene Based Polyurethane Binder System via FT-IR Measurements

Jiahua Guo ^{1,2} , Tao Chai ^{1,*}, Yucun Liu ^{1,*}, Jianlan Cui ¹, Hui Ma ^{1,*}, Suming Jing ¹, Lunchao Zhong ^{1,3}, Shengdong Qin ¹, Guodong Wang ^{1,4} and Xiang Ren ^{2,5,*}

¹ Chemical Engineering and Environment College, North University of China, Taiyuan 030051, China; guojiahuphd@163.com (J.G.); nuccjl@sina.com (J.C.); j782855067@163.com (S.J.); qiangshou302@sz.tsinghua.edu.cn (L.Z.); qsdnuc@sina.com (S.Q.); shiran1981@163.com (G.W.)

² Department of ESH, Science and Technology University of Sichuan Staff, Chengdu 610101, China

³ Graduate School at Shenzhen, Tsinghua University, Shenzhen 518000, China

⁴ School of Ammunition Engineering, Army Engineering University, Shijiazhuang 050003, China

⁵ College of Engineering, Sichuan Normal University, Chengdu 610101, China

* Correspondence: lyc2ct@sina.com (T.C.); lycnuc@sina.com (Y.L.); mahui20032011@163.com (H.M.); renxiang136@163.com (X.R.); Tel.: +86-288-481-8712 (T.C.)

Received: 5 April 2018; Accepted: 30 April 2018; Published: 4 May 2018



Abstract: Polyurethane binder systems based on hydroxyl-terminated polybutadiene (HTPB) possess several superior properties such as superior adhesion, high solid-loading capacity, outstanding mechanical performance, etc. They have been widely used in coatings and adhesives as well as in medical and military industries. The cure reaction between hydroxyl-terminated polybutadiene (HTPB) and diisocyanates plays a key role in the properties of final products as well as the adjustment of process parameters. FT-IR spectroscopy is applied to investigate the kinetics of the curing reaction of HTPB and isophorone diisocyanate (IPDI) in the presence of a low toxic and low viscosity catalyst, stannous isoctoate (TECH). The concentrations of the isocyanate groups (NCO) characterized by FT-IR during the cure reaction with respect to time were recorded at different temperatures and at constant stoichiometric ratio $R_{n[\text{NCO}]/n[\text{OH}]} = 1.0$. The kinetic parameters, i.e., activation energy (E_a), pre-exponential factor (A), activation enthalpy (ΔH) and activation entropy (ΔS) were determined. In addition, the curing process and mechanism of the HTPB-IPDI reaction are discussed.

Keywords: HTPB; binder; cure reaction; kinetics; mechanism

1. Introduction

Hydroxyl-terminated polybutadiene (HTPB) is a form of liquid telechelic rubber with different molecular weight (approximately 1500–10,000 g·mol⁻¹) and a high level of reactive functionality [1]. The liquid rubber possesses a unique combination of properties including a low glass transition temperature, low temperature flexibility, high solid-loading capacity, and excellent flow ability. They have been widely used in adhesives, coatings, sealants, medicine, as well as energetic materials [2–6]. As a result of the dimensional stability and structural integrity inherent from the cured polyurethane (PU) network, a HTPB-based binder system has found extensive applications in polymer-bonded explosives (PBXs), underwater weapons, composite solid propellants, and missile and launch vehicle technology [7–9]. The curing reaction of the polyurethane binder system which is based on HTPB and various diisocyanates (TDI Toluene diisocyanate, IPDI Isophorone diisocyanate, HDI Hexamethylene diisocyanate, etc.) to form a PU network (as shown in Figure 1), plays an important role in the manufacturing process as well as the properties of final products [9–13].

The kinetic reaction and mechanism of the cure reaction determine the physicochemical properties and mechanical performance of the cured product [14]. Therefore, knowledge of the kinetics of the polyurethane-curing reaction is of utmost importance for the design and preparation of specific products possessing suitable properties [15–17].

In recent years, several publications have reported on the research of the kinetics of PU formation through the use of viscosity buildup, ultrasonic waves, microcalorimetry, differential scanning calorimetry (DSC), Fourier-transform infrared spectroscopy (FTIR), and nuclear magnetic resonance (NMR) measurements [18–25]. Although there are several ways to study curing kinetics, FT-IR is known as a very rapid and reliable method well suited for monitoring the curing process of the PU formation. Such a test can reveal the extent of functional groups (such as the NCO group) consumption and during the cure reaction [21–25]. In this work, FT-IR measurement is applied to study the cure reaction of HTPB and IPDI with stannous isoctoate (TECH) as a catalyst. Through the study of the PU formation kinetics, an insight into the curing reaction may be obtained. In addition, the kinetic parameters, i.e., the pre-exponential factor (A), rate constant (k), activation energy (E_a), activation enthalpy (ΔH), and activation entropy (ΔS) for the cure reaction are calculated.

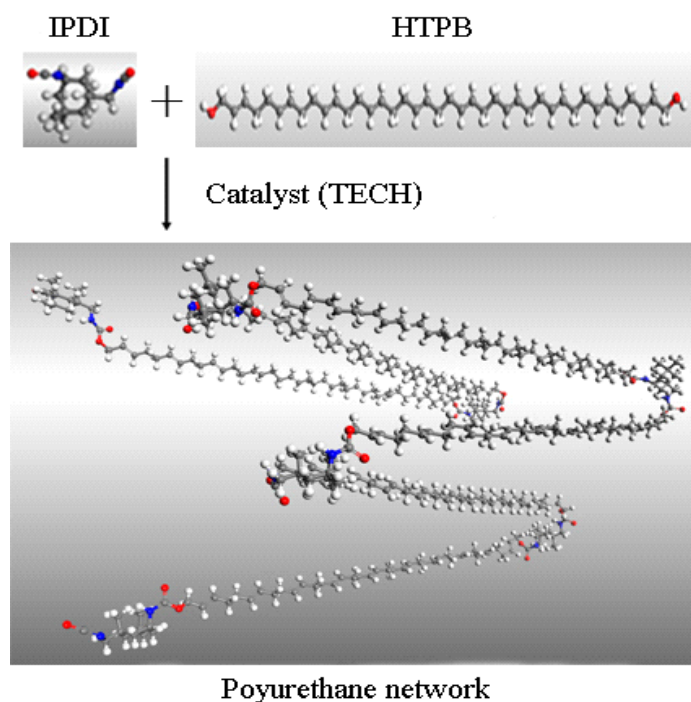


Figure 1. Schematic diagram of polyurethane network formation from HTPB and IPDI.

2. Materials and Methods

2.1. Materials

Hydroxyl-terminated polybutadiene (HTPB, number-average molecular weight = 2700, hydroxyl value = 45.2 mg KOH/g) was obtained from Liming Research Institute of Chemical Industry (Luoyang, China). Curing agent, isophorone diisocyanate (IPDI) was supplied by Bayer (Leverkusen, Germany). Catalyst, stannous isoctoate (TECH) was purchased from Sinopharm Chemical Reagent (Shanghai, China). Potassium bromide (KBr) was delivered by Merck (Darmstadt, Germany).

HTPB was dried under vacuum at 105 °C for 2 h then put under a nitrogen atmosphere before use. Other materials were used as received.

2.2. Sample Preparation

HTPB and IPDI were precisely weighed with a stoichiometric ratio $R_{n[\text{NCO}]/n[\text{OH}]} = 1.0$ then mixed for 2 min at high-speed stirring (2500 rpm) by a mechanical stirrer. At the beginning of the blending process, the corresponding amount of catalyst TECH was added to the system. The materials were mixed at room temperature and the concentration of the catalyst used in the binder system was 0.1 wt %. Having thoroughly blended all reactants, samples were prepared for immediate kinetic measurement. The polymerization reaction was performed not in anhydrous conditions and not under nitrogen atmosphere.

2.3. Fourier-Transform Infrared (FT-IR) Spectroscopy Analysis

The curing reaction between HTPB and IPDI was investigated by measuring the changes of the characteristic peaks of isocyanate groups ($\sim 2260 \text{ cm}^{-1}$) in the FT-IR spectroscopy. The infrared spectra of the samples were analyzed by a Perkin Elmer 100 Spectrometer (Waltham, MA, USA). Measurements were carried out by the transmittance mode in the range of $4000\text{--}400 \text{ cm}^{-1}$. Approximately 60 mg of crystalline KBr was pressed into a wafer with a diameter of 1.3 cm by exerting a pressure of 25 MPa for 1 min. A tiny drop of the binder mixture was coated between two KBr windows right after the sample was prepared. The samples measured in the FT-IR test were kept in a vacuum oven. The preset temperature was in the range of $35\text{--}75 \text{ }^\circ\text{C}$ with an accuracy of $\pm 0.1 \text{ }^\circ\text{C}$. The oven was located close to the FTIR Spectrometer to minimize thermal transients during the handling of the FT-IR wafer. The cure reaction was monitored by testing the infrared spectra of the sample at appropriate time intervals with respect to the reaction temperature.

3. Results and Discussion

3.1. Determination of the Reaction Rate Constants

The FT-IR spectra versus the time of the HTPB-IPDI curing reaction at $75 \text{ }^\circ\text{C}$ in the presence of TECH (0.1 wt %) as catalyst is shown in Figure 2.

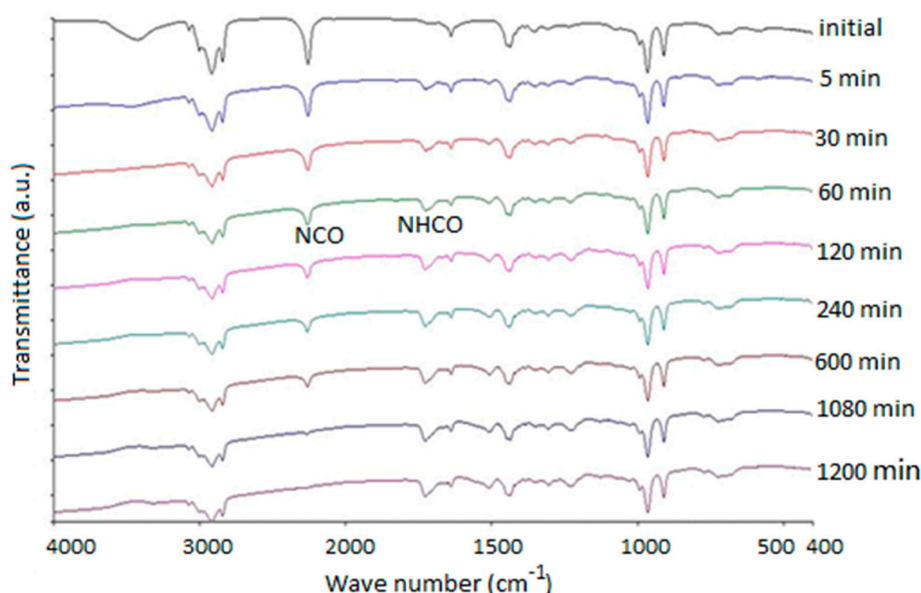


Figure 2. FT-IR spectra versus time of HTPB-IPDI reaction at $75 \text{ }^\circ\text{C}$ with TECH (0.1 wt %) as catalyst.

From the spectra, one can find that, as the reaction proceeded, the intensity of the characteristic peaks around 2260 cm^{-1} (NCO stretching) decreased and ultimately disappeared once the reaction was totally completed while the C=C stretching bands around 1640 cm^{-1} remained practically unaltered.

A new characteristic absorption peak in the unique range of 1710–1760 cm^{-1} was attributed to the C=O stretching vibration, which confirmed the formation of the polyurethane group during the cure reaction [25]. To ensure that the quantitative results were independent of the thickness of the sample between two KBr wafers, the change in the intensity of the NCO stretching band of IPDI at 2260 cm^{-1} was monitored and divided by the intensity of the reference band at 1640 cm^{-1} for the C=C stretching in HTPB [21]. According to the Lambert-Beer law, a given peak area is directly proportional to the reagent concentration. Thus, the conversion of NCO can be derived from the FT-IR spectra recorded as a function of time, which can be calculated from the FT-IR data as [25]:

$$P_{\text{NCO}} = \frac{\left(\frac{C_{2260}}{C_{1640}}\right)_{T=0} - \left(\frac{C_{2260}}{C_{1640}}\right)_{T=t}}{\left(\frac{C_{2260}}{C_{1640}}\right)_{T=0}} \quad (1)$$

where P_{NCO} represents the conversion of isocyanate groups, C represents the absorbance values at 2260 cm^{-1} /1640 cm^{-1} in the FT-IR spectra, and the subscripts of 0 and t denote reaction times.

The rate constant for the PU formation between HTPB and IPDI was obtained from the slope of the straight line by plotting the $P/(1 - P)$ versus time according to the following equation [26]:

$$\frac{P_{\text{NCO}}}{1 - P_{\text{NCO}}} = k t \quad (2)$$

where P_{NCO} is the conversion of NCO group, k is the rate constant, t is the curing time.

Five different temperatures (from 35 °C to 75 °C) were conducted to calculate the kinetic parameters of the curing reaction, as shown in Figure 3.

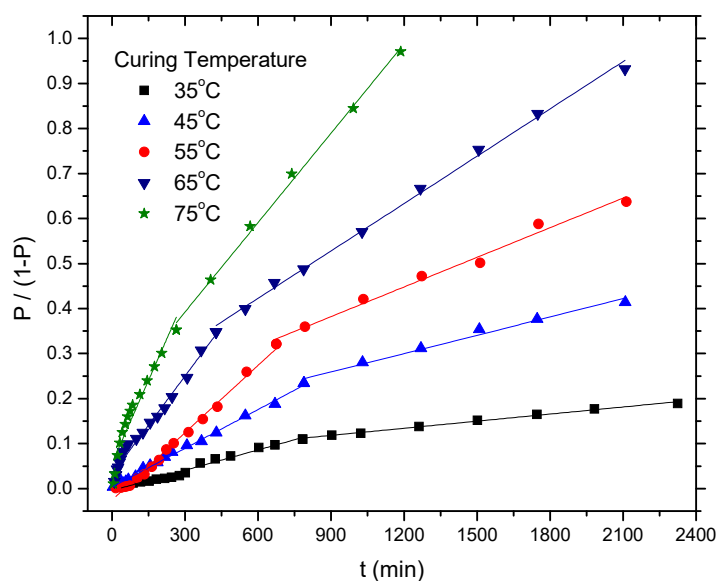


Figure 3. The plot of $P/(1 - P)$ versus time at various curing temperatures for the HTPB-IPDI binder system.

Clearly, the profile of the cure reaction of the HTPB-IPDI binder system showed a discontinuity at each temperature. Two steps were featured, which included a faster initial step (i.e., Step 1 with a rate constant k_1) and a slower consecutive step (i.e., Step 2 with a rate constant k_2). The corresponding data for both steps are listed in Table 1.

Table 1. Rate constants for the polymerization of HTPB-IPDI system at different isothermal curing temperatures in the presence of TECH (0.1 wt %) as catalyst.

| T (°C) | $k_1 \cdot 10^3$ (min ⁻¹) | R-Square | $k_2 \cdot 10^3$ (min ⁻¹) | R-Square | $k_{1(T)}/k_{1(35)}$ | $k_{2(T)}/k_{2(35)}$ | k_1/k_2 |
|----------|---------------------------------------|----------|---------------------------------------|----------|----------------------|----------------------|-----------|
| 35 | 0.1503 | 0.9764 | 0.0519 | 0.9948 | 1.00 | 1.00 | 2.89 |
| 45 | 0.2871 | 0.9960 | 0.1356 | 0.9791 | 1.91 | 2.61 | 2.12 |
| 55 | 0.4850 | 0.9890 | 0.2338 | 0.9761 | 3.23 | 4.50 | 2.07 |
| 65 | 0.7177 | 0.9668 | 0.3578 | 0.9948 | 4.77 | 6.89 | 2.01 |
| 75 | 1.2300 | 0.9482 | 0.6618 | 0.9962 | 8.18 | 12.74 | 1.86 |

T = Curing Temperature; k_1, k_2 = rate constant for step 1 and step 2 from FT-IR measurement.

The differences in the rate constants in different steps indicate that the polymerization between HTPB and IPDI obeyed second-order kinetics. Notably, both constants (k_1, k_2) increase with the increase of curing temperature from 35 °C to 75 °C.

On the other hand, the ratio of k_1/k_2 showed a decreasing trend as the temperature increased, from 2.89 (35 °C) decreased to 1.86 (75 °C). This result is similar to Lucio's research [14], in the presence of (ferrocenylbutyl) dimethylsilane, the ratio of k_1/k_2 for HTPB-IPDI system decreased from 2.39 (50 °C) to 1.60 (80 °C). From the ratio of $k_{1(T)}/k_{1(35)}$ and $k_{2(T)}/k_{2(35)}$, the catalytic effect in Step 2 was pronounced than that of Step 1 with the an increase in curing temperature. For example, the value of $k_{1(75)}/k_{1(35)}$ was 8.18, whereas $k_{2(75)}/k_{2(35)}$ was 12.74. The results indicate that k_2 was more sensitive to the curing reaction temperature in the presence of catalyst TECH. In other words, when the curing temperature increased, k_2 increased higher than k_1 . This behavior may have been attributable to the catalytic activity of the organometallic compound (such as TECH) on the different NCO groups (such as primary NCO and secondary NCO) which was not identical. The addition of this type of catalyst may have expanded the disparity of the reactivity of the non-equivalence NCO groups in the asymmetric diisocyanates (such as IPDI and TDI) and, consequently, the rate constants of the two steps in the cure reaction were different. In the previous literature, similar behavior was also observed by Burel, whose research involved an analogous system in the presence of dibutyltin dilaurate (DBTDL) as catalyst [23].

3.2. Kinetic Studies by FT-IR Measurements

The thermodynamic parameters, such as pre-exponential factor (A), activation energy (E_a), activation entropy (ΔS), and activation enthalpy (ΔH), were determined from the Arrhenius equation and Eyring equation:

$$\ln k = -\frac{E_a}{RT} + \ln A \quad (3)$$

$$\ln \frac{k}{T} = -\frac{\Delta H}{RT} + \frac{\Delta S}{R} + \ln \frac{R}{Nh} \quad (4)$$

where k is the reaction constant, T is the curing temperature (K), R is the universal gas constant ($R = 8.314 \text{ J}\cdot\text{mol}^{-1}\cdot\text{K}^{-1}$), N is Avogadro constant ($N = 6.022 \times 10^{23} \text{ mol}^{-1}$) and, h is Planck constant ($h = 6.626 \times 10^{-34} \text{ J}\cdot\text{s}$).

From the Arrhenius plot (Figure 4a), the activation energy (E_a) and pre-exponential factor (A) are computed with a first-order liner fitting. A similar evaluation of the kinetic data in the Eyring plot (Figure 4b) was adopted to obtain the value of activation entropy (ΔS) and activation enthalpy (ΔH). The values of $A, E_a, \Delta S$, and ΔH are computed and listed in Table 2.

Table 2. Thermodynamic parameters for the reaction of HTPB-IPDI system.

| E_{a1} | E_{a2} | A_1 | A_2 | ΔH_1 | ΔH_2 | ΔS_1 | ΔS_2 |
|-------------------------|-------------------------|---|---|-------------------------|-------------------------|---|---|
| (kJ·mol ⁻¹) | (kJ·mol ⁻¹) | (L·mol ⁻¹ ·min ⁻¹) | (L·mol ⁻¹ ·min ⁻¹) | (kJ·mol ⁻¹) | (kJ·mol ⁻¹) | (J·mol ⁻¹ ·K ⁻¹) | (J·mol ⁻¹ ·K ⁻¹) |
| 45.80 | 54.23 | 8854 | 92,745 | 43.01 | 53.51 | -178.44 | -158.91 |

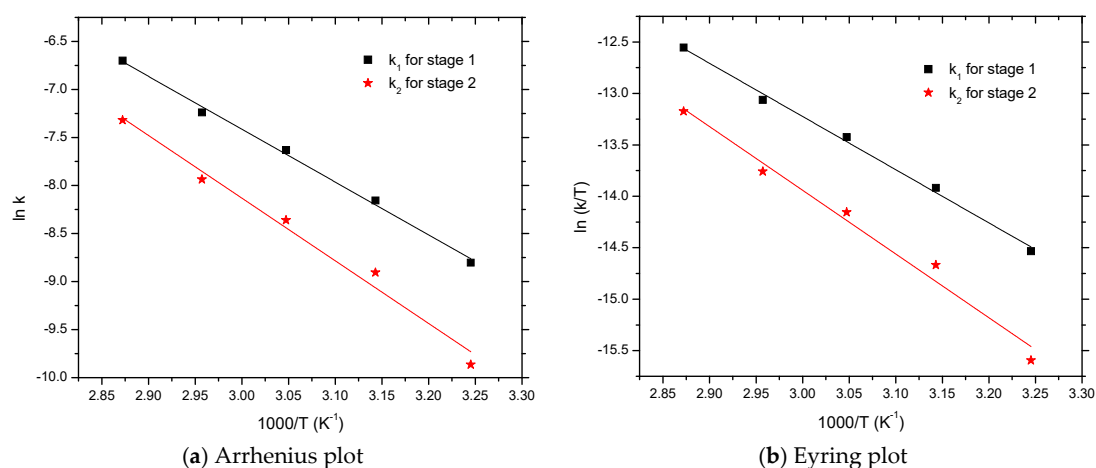


Figure 4. Arrhenius and Eyring plots for the curing reaction between HTPB and IPDI.

As seen in Table 2, the activation energy of E_{a1} ($45.80 \text{ kJ}\cdot\text{mol}^{-1}$) was lower than E_{a2} ($54.23 \text{ kJ}\cdot\text{mol}^{-1}$), relating to its faster urethane reaction rate k_1 which was much higher than k_2 . The pre-exponential factor (also called frequency factor) for Step 1 was approximately $A_1 = 8854$, and $A_2 = 92,745$ for the Step 2. One explanation may have been the kinetic control mechanism which caused the cure reaction between IPDI and HTPB in the initial step (Step 1); concurrently in the subsequent step (Step 2), the reaction was largely governed by a diffusion process [24].

As seen in Table 2, the activation enthalpy was found to be $43.01 \text{ kJ}\cdot\text{mol}^{-1}(\Delta H_1)$ and $51.51 \text{ kJ}\cdot\text{mol}^{-1}(\Delta H_2)$. The activation entropy for the Step 1 was about $\Delta S_1 = -178.44 \text{ J}\cdot\text{mol}^{-1}\cdot\text{K}^{-1}$, and $\Delta S_2 = -158.91 \text{ J}\cdot\text{mol}^{-1}\cdot\text{K}^{-1}$ for the Step 2. Clearly, activation enthalpy and entropy values are useful to reveal the mechanism. In transition-state theory, activation entropy is usually considered as the degree of disorder in the reaction system [27]. Large negative values of the activation entropy indicate that energy must be partitioned into a lesser state at the transition-state, which illustrates an associative mechanism [28]. In comparison to the activation entropy values of the two steps, a larger negative value of ΔS_1 was found, which was related to the easier formation of the transition state.

3.3. Analysis of Curing Mechanism of HTPB-IPDI Binder System

To understand the causes of the two-step phenomenon which occurred during the curing reaction between HTPB and IPDI, two aspects need to be analyzed. Firstly, one must consider the chemical structures of the HTPB and IPDI used in the experiment. Generally, a HTPB microstructure comprises of approximately 60% *trans*-1,4-structure, 20% *cis*-1,4-structure and 20% *vinyl*-1,2-structure [1]. In theory, the reactivity of OH groups in HTPB should be different. However, thanks to the relatively large molecular weight, the reactivity of all OH groups in HTPB were largely similar and were not likely to cause significant differences in reaction rates. The other reactant of the curing system was IPDI, which possesses two asymmetric NCO groups, as shown in Figure 5a. The commercial IPDI usually contains a ratio of 25%~30% *trans*-isomer and 70%~75% *cis*-isomer, thus, there are two non-equivalent NCO groups were in four unequal positions [29], as shown in Figure 5b.

As a result, only the structure of IPDI, the eight different products, and eight rate constants needed be considered. It is obviously that the PU formation of IPDI and HTPB was too complex to analyze if no assumptions were made to simplify the reaction system [14]. Fortunately, according to the study of Rochery, the main position of secondary NCO group was in the horizontal direction, therefore, the major isomer of IPDI was *cis*-horizontal-NCO_{sec}, as shown in Figure 5b with ellipses [29]. The relative reactivity of NCO groups in IPDI could be simplified and attention was focused on the difference in activity between primary NCO and secondary NCO. As a result of the larger steric effect of the cyclohexane ring and *a*-substituted methyl, the reactivity of primary NCO was much lower than secondary NCO.

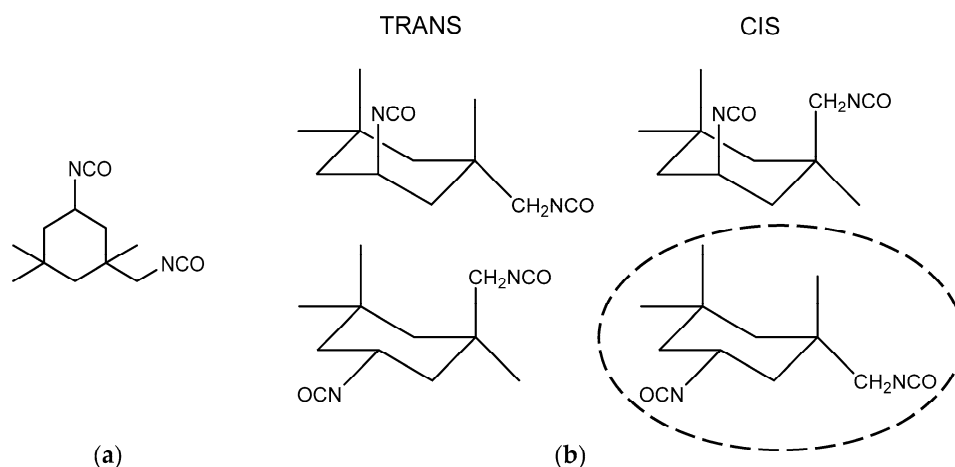


Figure 5. Structure of (a) IPDI and (b) four isomers of IPDI.

On the other hand, it was important to interpret all the reactions including simultaneous and competitive reactions which occurred during the two steps. From the experimental phenomenon and the simplified assumptions of HTPB and IPDI, we proposed the reaction mechanism of HTPB-IPDI binder system, as shown in Figure 6. There were two main steps in the curing process of HTPB-IPDI binder system. In Step 1, two moles of secondary NCO groups in IPDI reacted with two OH groups in one mole HTPB. At the beginning of the curing reaction, the rate constant k_1 was relatively large, mainly caused by kinetic control mechanism. In Step 2, the primary NCO groups in IPDI reacted with OH groups in HTPB and formed a three-dimensional network structure polyurethane, given the rate constant k_2 in this step is relatively small.

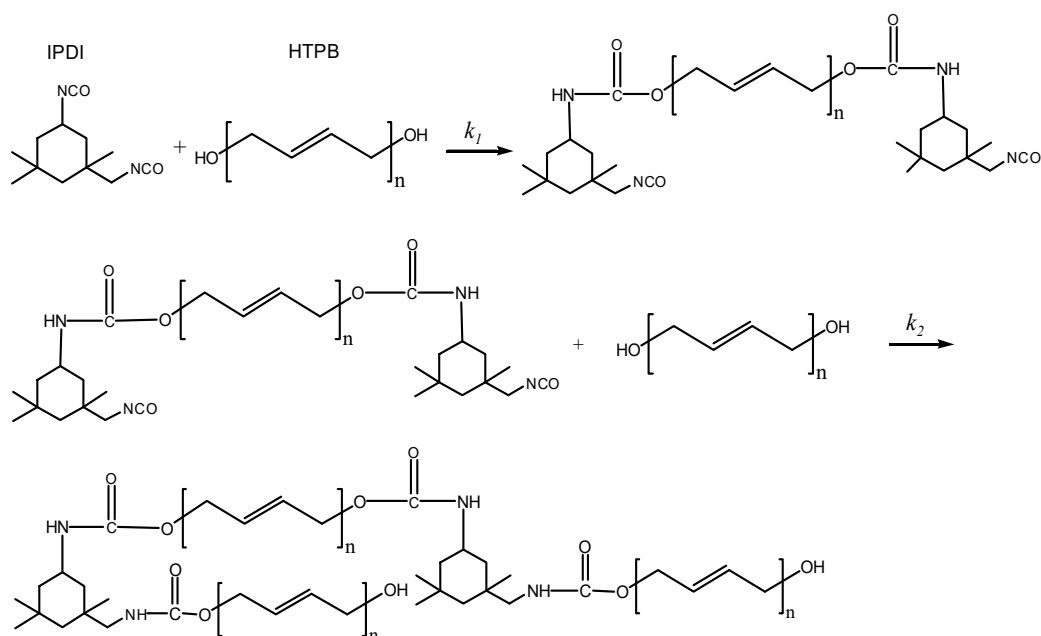


Figure 6. Curing process of HTPB-IPDI binder system.

4. Conclusions

In this work, FT-IR was applied to monitor the cure reaction of HTPB and IPDI with TECH used as a catalyst. The presence of two steps in the polyurethane formation was clearly observed, the rate constant was different in the first and second steps in all curing temperatures. Since experimental results showed

two broken lines, accordingly, all the other results are followed this trend. Other kinetic parameters, such as activation energy (E_a), activation entropy (ΔS), and activation enthalpy (ΔH), were determined from the Arrhenius formula and Eyring equation. All parameters had two values, with each standing for different steps of the curing reaction. This phenomenon was largely attributable to the two asymmetric isocyanate groups in IPDI, which was expected to lead to two different polymerization rates.

Author Contributions: T.C. and Y.L. conceived and designed the experiments; J.G., H.M., J.C., S.J., L.Z. and S.Q. performed the experiments; H.M. analyzed the data; G.W. and X.R. contributed reagents/materials/analysis tools; J.G. and H.M. wrote the paper.

Funding: This work was supported by NSAF (Grant No. U1330131) and Sichuan Safety Supervision Bureau Safety Production Technology Project (Grant No. aj20170518104846).

Conflicts of Interest: The authors declare no conflict of interest.

References

1. Krishnan, P.S.G.; Ayyaswamy, K.; Nayak, S. Hydroxy terminated polybutadiene: Chemical modifications and applications. *J. Macromol. Sci. Part A* **2013**, *50*, 128–138. [[CrossRef](#)]
2. Dey, A.; Athar, J.; Varma, P.; Prasant, H.; Sikder, A.K.; Chattopadhyay, S. Graphene-iron oxide nanocomposite (GINC): An efficient catalyst for ammonium perchlorate (AP) decomposition and burn rate enhancer for AP based composite propellant. *RSC Adv.* **2015**, *5*, 1950–1960. [[CrossRef](#)]
3. Florczak, B. Viscosity Testing of HTPB Rubber Based Pre-binders. *Cent. Eur. J. Energ. Mater.* **2014**, *11*, 625–637.
4. Amrollahi, M.; Sadeghi, G.M.M.; Kashcooli, Y. Investigation of novel polyurethane elastomeric networks based on polybutadiene-ol/polypropyleneoxide mixture and their structure-properties relationship. *Mater. Des.* **2011**, *32*, 3933–3941. [[CrossRef](#)]
5. Sheikhy, H.; Shahidzadeh, M.; Ramezanzadeh, B.; Noroozi, F. Studying the effects of chain extenders chemical structures on the adhesion and mechanical properties of a polyurethane adhesive. *J. Ind. Eng. Chem.* **2013**, *19*, 1949–1955. [[CrossRef](#)]
6. Xia, W.; Zhu, N.; Hou, R.; Zhong, W.; Chen, M. Preparation and characterization of fluorinated hydrophobic UV-crosslinkable thiol-ene polyurethane coatings. *Coatings* **2017**, *7*, 117. [[CrossRef](#)]
7. Gohardani, A.S.; Stanojev, J.; Demairé, A.; Anflo, K.; Persson, M.; Wingborg, N.; Nilsson, C. Green space propulsion: Opportunities and prospects. *Prog. Aeronaut. Sci.* **2014**, *71*, 128–149. [[CrossRef](#)]
8. Li, H.X.; Wang, J.Y.; An, C.W. Study on the rheological properties of CL-20/HTPB casting explosives. *Cent. Eur. J. Energ. Mater.* **2014**, *11*, 237–255.
9. Cumming, A.S. New trends in advanced high energy materials. *J. Aerosp. Technol. Manag.* **2009**, *1*, 161–166. [[CrossRef](#)]
10. Wang, Z.; Qiang, H.; Wang, G.; Wang, T. A new test method to obtain biaxial tensile behaviors of solid propellant at high strain rates. *Iran. Polym. J.* **2016**, *25*, 515–524. [[CrossRef](#)]
11. Shekhar, H.; Sahasrabudhe, A.D. Longitudinal strain dependent variation of Poisson's ratio for HTPB based solid rocket propellants in uni-axial tensile testing. *Propellants Explos. Pyrotech.* **2011**, *36*, 558–563. [[CrossRef](#)]
12. DeLuca, L.T.; Galfetti, L.; Maggi, F.; Colombo, G.; Merotto, L.; Boiocchi, M.; Paravan, C.; Reina, A.; Tadini, P.; Fanton, L. Characterization of HTPB-based solid fuel formulations: Performance, mechanical properties, and pollution. *Acta Astronaut.* **2013**, *92*, 150–162. [[CrossRef](#)]
13. Ma, H.; Liu, Y.C.; Chai, T.; Hu, T.P.; Guo, J.H.; Yu, Y.W.; Yuan, J.M.; Wang, J.H.; Qin, N.; Zhang, L. Kinetic studies on the cure reaction of hydroxyl-terminated polybutadiene based polyurethane with variable catalysts by differential scanning calorimetry. *e-Polymers* **2017**, *17*, 89–94.
14. Lucio, B.; de la Fuente, J.L. Rheokinetic analysis on the formation of metallo-polyurethanes based on hydroxyl-terminated polybutadiene. *Eur. Polym. J.* **2014**, *50*, 117–126. [[CrossRef](#)]
15. Rao, M.R.; Scariah, K.; Varghese, A.; Naik, P.; Swamy, K.N.; Sastri, K. Evaluation of criteria for blending hydroxy terminated polybutadiene (HTPB) polymers based on viscosity build-up and mechanical properties of gumstock. *Eur. Polym. J.* **2000**, *36*, 1645–1651.
16. Varghese, A.; Scariah, K.; Bera, S.; Rao, M.R.; Sastri, K. Processability characteristics of hydroxy terminated polybutadienes. *Eur. Polym. J.* **1996**, *32*, 79–83. [[CrossRef](#)]

17. Lee, S.; Choi, J.H.; Hong, I.-K.; Lee, J.W. Curing behavior of polyurethane as a binder for polymer-bonded explosives. *J. Ind. Eng. Chem.* **2015**, *21*, 980–985. [[CrossRef](#)]
18. Bina, C.K.; Kannan, K.; Ninan, K. DSC study on the effect of isocyanates and catalysts on the HTPB cure reaction. *J. Therm. Anal. Calorim.* **2004**, *78*, 753–760. [[CrossRef](#)]
19. Xiao, Y.; Jin, B.; Peng, R.; Zhang, Q.; Liu, Q.; Guo, P.; Chu, S. Kinetic and thermodynamic analysis of the hydroxyl-terminated polybutadiene binder system by using microcalorimetry. *Thermochim. Acta* **2018**, *659*, 13–18. [[CrossRef](#)]
20. Zhao, J.; Zhang, A.; Luo, Z.; Zhu, H.; Zeng, F.; Zhou, X.; Xie, X. On-line monitoring the curing behaviors of hydroxyl-terminated polybutadiene/toluene diisocyanate system via ultrasonic wave. *J. Funct. Mater.* **2011**, *9*, 1649–1652.
21. Kincal, D.; Ozkar, S. Kinetic study of the reaction between hydroxyl-terminated polybutadiene and isophorone diisocyanate in bulk by quantitative FTIR spectroscopy. *J. Appl. Polym. Sci.* **1997**, *66*, 1979–1984. [[CrossRef](#)]
22. Yang, P.F.; Yu, Y.H.; Wang, S.P.; Li, T.D. Kinetic studies of isophorone diisocyanate-polyether polymerization with in situ FT-IR. *Int. J. Polym. Anal. Charact.* **2011**, *16*, 584–590. [[CrossRef](#)]
23. Burel, F.; Feldman, A.; Bunel, C. Hydrogenated hydroxy-functionalized polyisoprene (H-HTPI) and isocyanurate of isophorone diisocyanates (I-IPDI): Reaction kinetics study using FTIR spectroscopy. *Polymer* **2005**, *46*, 15–25. [[CrossRef](#)]
24. Hailu, K.; Guthausen, G.; Becker, W.; König, A.; Bendfeld, A.; Geissler, E. In-situ characterization of the cure reaction of HTPB and IPDI by simultaneous NMR and IR measurements. *Polym. Test.* **2010**, *29*, 513–519. [[CrossRef](#)]
25. Han, J.; Yu, C.; Lin, Y.; Hsieh, K. Kinetic study of the urethane and urea reactions of isophorone diisocyanate. *J. Appl. Polym. Sci.* **2008**, *107*, 3891–3902. [[CrossRef](#)]
26. Vancaeyzeele, C.; Fichet, O.; Laskar, J.; Boileau, S.; Teyssié, D. Polyisobutene/polystyrene interpenetrating polymer networks: Effects of network formation order and composition on the IPN architecture. *Polymer* **2006**, *47*, 2046–2060. [[CrossRef](#)]
27. Espenson, J.H. *Chemical Kinetics and Reaction Mechanisms*, 2nd ed.; McGraw-Hill: New York, NY, USA, 1995.
28. Fatemeh, G.; Sayyed, M.H.K.; Mehdi, S. Kinetic spectrophotometric method for the 1,4-diionic organophosphorus formation in the presence of Meldrum's Acid: Stopped-flow approach. *Molecules* **2016**, *21*, 1514.
29. Rochery, M.; Vroman, I.; Lam, T.M. Kinetic model for the reaction of IPDI and macrodiols: Study on the relative reactivity of isocyanate groups. *J. Macromol. Sci. Part A* **2000**, *37*, 259–275. [[CrossRef](#)]



© 2018 by the authors. Licensee MDPI, Basel, Switzerland. This article is an open access article distributed under the terms and conditions of the Creative Commons Attribution (CC BY) license (<http://creativecommons.org/licenses/by/4.0/>).